



**HAL**  
open science

## Optimization and Prediction of Stability of Emulsified Liquid Membrane (ELM): Artificial Neural Network

Meriem Zamouche, Hichem Tahraoui, Zakaria Laggoun, Sabrina Mechat, Rayene Chemchmi, Muhammad Imran Kanjal, Abdeltif Amrane, Amina Hadadi, Lotfi Mouni

### ► To cite this version:

Meriem Zamouche, Hichem Tahraoui, Zakaria Laggoun, Sabrina Mechat, Rayene Chemchmi, et al.. Optimization and Prediction of Stability of Emulsified Liquid Membrane (ELM): Artificial Neural Network. Processes, 2023, 11 (2), pp.364. 10.3390/pr11020364 . hal-03975991

**HAL Id: hal-03975991**

**<https://hal.science/hal-03975991v1>**

Submitted on 30 May 2023

**HAL** is a multi-disciplinary open access archive for the deposit and dissemination of scientific research documents, whether they are published or not. The documents may come from teaching and research institutions in France or abroad, or from public or private research centers.

L'archive ouverte pluridisciplinaire **HAL**, est destinée au dépôt et à la diffusion de documents scientifiques de niveau recherche, publiés ou non, émanant des établissements d'enseignement et de recherche français ou étrangers, des laboratoires publics ou privés.



Distributed under a Creative Commons Attribution 4.0 International License

## Article

# Optimization and Prediction of Stability of Emulsified Liquid Membrane (ELM): Artificial Neural Network

Meriem Zamouche <sup>1,\*</sup>, Hichem Tahraoui <sup>2</sup>, Zakaria Laggoun <sup>1</sup>, Sabrina Mechaty <sup>1</sup>, Rayene Chemchmi <sup>1</sup>, Muhammad Imran Kanjal <sup>3</sup>, Abdeltif Amrane <sup>4</sup>, Amina Hadadi <sup>5</sup> and Lotfi Mouni <sup>5,\*</sup>

<sup>1</sup> Department of Environmental Engineering/Laboratoire de Recherche sur le Médicament et le Développement Durable (ReMeDD), University of Salah Boubnider Constantine 3, El Khroub 25012, Algeria

<sup>2</sup> Laboratory of Biomaterials and Transport Phenomena (LBMP), University of Médéa, Médéa 26000, Algeria

<sup>3</sup> Department of Chemistry, Government College University, Faisalabad 38000, Pakistan

<sup>4</sup> University Rennes, Ecole Nationale Supérieure de Chimie de Rennes, CNRS, ISCR—UMR6226, F-35000 Rennes, France

<sup>5</sup> Laboratory of Management and Valorization of Natural Resources and Quality Assurance, SNVST Faculty, Akli Mohand Oulhadj University, Bouira 10000, Algeria

\* Correspondence: meriem.zamouche@univ-constantine3.dz (M.Z.); l.mouni@univ-bouira.dz (L.M.)

**Abstract:** In this work, the emulsified liquid membrane (ELM) extraction process was studied as a technique for separating different pollutants from an aqueous solution. The emulsified liquid membrane used consisted of Sorbitan mono-oleate (Span 80) as a surfactant with n-hexane (C<sub>6</sub>H<sub>14</sub>) as a diluent; the internal phase used was nitric acid (HNO<sub>3</sub>). The major constraint in the implementation of the extraction process by an emulsified liquid membrane (ELM) is the stability of the emulsion. However, this study focused first on controlling the stability of the emulsion by optimizing many operational factors, which have a direct impact on the stability of the membrane. Among the important parameters that cause membrane breakage, the surfactant concentration, the emulsification time, and the stirring speed were demonstrated. The optimization results obtained showed that the rupture rate (Tr) decreased until reaching a minimum value of 0.07% at 2% of weight/weight of Span 80 concentration with an emulsification time of 3 min and a stirring speed of 250 rpm. On the other hand, the volume of the inner phase leaking into the outer phase was predicted using an artificial neural network (ANN). The evaluation criteria of the ANN model in terms of statistical coefficient and RMSE error revealed very interesting results and the performance of the model since the statistical coefficients were very high and close to 1 in the four phases (R<sub>training</sub> = 0.99724; R<sub>validation</sub> = 0.99802; R<sub>test</sub> = 0.99852; R<sub>all data</sub> = 0.99772), and also, statistical errors of RMSE were minimal (RMSE<sub>training</sub> = 0.0378; RMSE<sub>validation</sub> = 0.0420; RMSE<sub>test</sub> = 0.0509; RMSE<sub>all data</sub> = 0.0406).

**Keywords:** emulsified liquid membrane (ELM); stability; Span 80; stirring speed; emulsification time; artificial neural network



**Citation:** Zamouche, M.; Tahraoui, H.; Laggoun, Z.; Mechaty, S.; Chemchmi, R.; Kanjal, M.I.; Amrane, A.; Hadadi, A.; Mouni, L. Optimization and Prediction of Stability of Emulsified Liquid Membrane (ELM): Artificial Neural Network. *Processes* **2023**, *11*, 364. <https://doi.org/10.3390/pr11020364>

Academic Editor: Yue Li

Received: 27 December 2022

Revised: 15 January 2023

Accepted: 20 January 2023

Published: 24 January 2023



**Copyright:** © 2023 by the authors. Licensee MDPI, Basel, Switzerland. This article is an open access article distributed under the terms and conditions of the Creative Commons Attribution (CC BY) license (<https://creativecommons.org/licenses/by/4.0/>).

## 1. Introduction

Solvent extraction (SE) has been widely used for heavy metal recovery [1–3] from aqueous solutions, particularly the extraction of noble and rare metals by using different extracting solvents. There are several applications of metal solvent extraction in the literature, such as extraction of Ti, Fe, Zn, Cu, Mn, Co, Ni, Li, Sc, Al, Ca, Ta, Nb, and U [4–10].

Solvent extraction is not the only process used to eliminate heavy metals from wastewater. Several techniques have also been used: chemical precipitation, ion exchange, coagulation, flocculation, cementation, adsorption, chelation, electrochemical processes, and photocatalytic precipitation [11–15]. These techniques, however, have certain limits. The ion exchange process is easy to use, but the weakness of the process is related to the encrustation of the resin, and its regeneration generates secondary pollution [14,16]. The

drawback of the electrochemical approach is the deposition rate and the solution composition [17]. Furthermore, this procedure requires substantial capital expenditure and a costly power supply. Chemical precipitation and adsorption generate sludge that presents a nuisance of waste [14]. In addition, these processes have slow mass transfer rates and lower efficiency with a high investment cost [14].

Solvent extraction is carried out by combining a solution containing the pollutants to be extracted with an organic solvent that often consists of an extractant and diluent and preferentially extracts one or more pollutants. This approach is dependent on the use of large quantities of organic solvent, which reflects process limitations, particularly when dealing with diluted solutions [1,18,19]. Moreover, organic solvents are often expensive, which explains the high cost of solvent extraction [1,19].

Various beneficial organic and inorganic components have been extracted and recovered from aqueous solutions via the application of various extraction techniques in recent years [20], which are solid phase extraction (SPE), liquid-liquid extraction (LLE) and membrane extraction (ME) [3,21].

The principle of the liquid membrane extraction process is based on the use of a liquid barrier in substitution of the solid one as membrane material between the two phases, the external phase containing the pollutant to be extracted and the internal phase [22]. In addition, The ELM technique integrates the extraction and stripping processes into a single step, therefore simultaneously purifying and concentrating the solute [23].

Emulsified liquid membrane (ELM) technology has been introduced through the further development of the liquid membrane method [22]. Li developed the ELM method in 1988; it is a promising technique for water treatment owing to its simplicity, selectivity separation, and high efficiency [2,20,24]. Since then, many papers have been published on the removal, recovery, and purification of numerous organic and inorganic chemicals from aqueous solutions, in addition to biological and medicinal uses. [25,26].

ELM was promising in the extraction of various metal ions such as  $\text{Ni}^{+2}$ ,  $\text{Cr}^{+3}$ ,  $\text{Mn}^{+2}$ ,  $\text{Co}^{+2}$ ,  $\text{Cu}^{+2}$ ,  $\text{Cr}^{+6}$ ,  $\text{Cd}^{+2}$ , and  $\text{Zn}^{+2}$  [27–31]. In addition to the recovery of rare earth (RE) and precious metals [26,32–37]. Other pollutants, which are hazardous to the environment, have been successfully extracted by ELM, such as phenols and chlorophenols [38–40], dyes [41–46], and pharmaceutical compounds [21,47–50]

ELMs are double emulsions; they are either water/oil/water (W/O/W) or oil/water/oil (O/W/O) systems [51]. First, an ELM for the  $W_1/O/W_2$  system is produced by combining two immiscible phases and then dispersing the resultant emulsion ( $W_1/O$ ) in a batch reactor comprising an external phase [22]. The external phase is called the feed phase, while the internal phase is known as the stripping phase.

The ELM separation procedure may be carried out in four stages, the first of which is emulsion preparation. The emulsion is made by combining the membrane and internal phases as water in oil ( $W_1/O$ ) [52]. The emulsion is composed of tiny aqueous droplets ( $W_1$ ) scattered throughout the organic membrane phase (O), resulting in globules of ( $W_1-O$ ) [22,52]. The second step consists in mixing the emulsion obtained before with the external aqueous phase to form a water-in-oil-in-water emulsion ( $W_1/O/W_2$ ) [52]. The third step consists of the permutation of the solute from the feed phase to the internal phase through the membrane. At the end of the extraction process, the  $W_1/O$  emulsion is separated from the purified feed phase by decantation. The last step is de-emulsification, which consists in separating the stripping (internal) phase from the membrane phase [52]. The recover membrane phase can be used for a further extraction process.

An emulsion requires the use of reagents such as an emulsifier, a carrier, and a diluent, but the surfactant is needed to stabilize W/O emulsions [23].

Due to the instability of the emulsion over a prolonged contact period, the implementation of ELM on an industrial scale has been restricted despite the advantages it provides in an extraction separation process. Emulsion stability is, therefore, the most crucial and limiting factor influencing the extraction procedure [53]. Therefore, it is important to study the parameters influencing the stability of the membrane before its use.

The main parameters influencing the stability of ELM are often the concentration of the surfactant, the type and the concentration of the internal phase reagent, type of diluent, ratio of internal phase volume to the membrane, emulsification time, and ratio of the emulsified liquid membrane volume to the feed phase.

Thus, the purpose of this study was to evaluate the effect of some parameters on the stability of the ELM constituted by  $\text{HNO}_3$  as the internal phase, Span 80 as a surfactant with n-hexane as a diluent, and the external phase as distilled water.

The parameters considered were surfactant concentration, emulsification time, concentration of internal phase, ratio of internal phase volume to the membrane, ratio of the emulsified liquid membrane volume to the feed phase, and stirring speed. Subsequently, the artificial neural network was used to predict the volume of the inner phase escaping into the outer phase. To our knowledge, such work has never been performed before.

## 2. Materials and Methods

### 2.1. Reagents

The Sorbitan mono-oleate (Span 80) ( $\text{C}_{24}\text{H}_{44}\text{O}_6$ ) and nitric acid ( $\text{HNO}_3$ ) 65% were obtained from Sigma-Aldrich. The n-hexane ( $\text{C}_6\text{H}_{14}$ ) (99%) was supplied from Biochem Chemopharma.

### 2.2. Emulsion Preparation

The emulsion was prepared in two emulsification steps:

The organic phase (membrane phase) was prepared by mixing 2% of weight/weight of Span 80 as a surfactant with 20 mL of n-hexane as diluent under moderate stirring (200 rpm) using a stirring plate (DLAB OS40-Pro, Ontario, City of industry, CA, USA). A volume of 20 mL of nitric acid solution ( $\text{HNO}_3$ ) at a concentration of 0.5M was used as an internal aqueous solution. In a 600 mL beaker, the emulsion was prepared by quickly mixing the two prior phases with a known volume ratio of 1/1 (Figure 1). To achieve such a high speed, a Bosch arm mixer (Gerlingen, Germany) was used, and stirring lasted three minutes. The volume ratio between the internal aqueous phase and the organic phase was adjusted from 1/2 to 3/2.

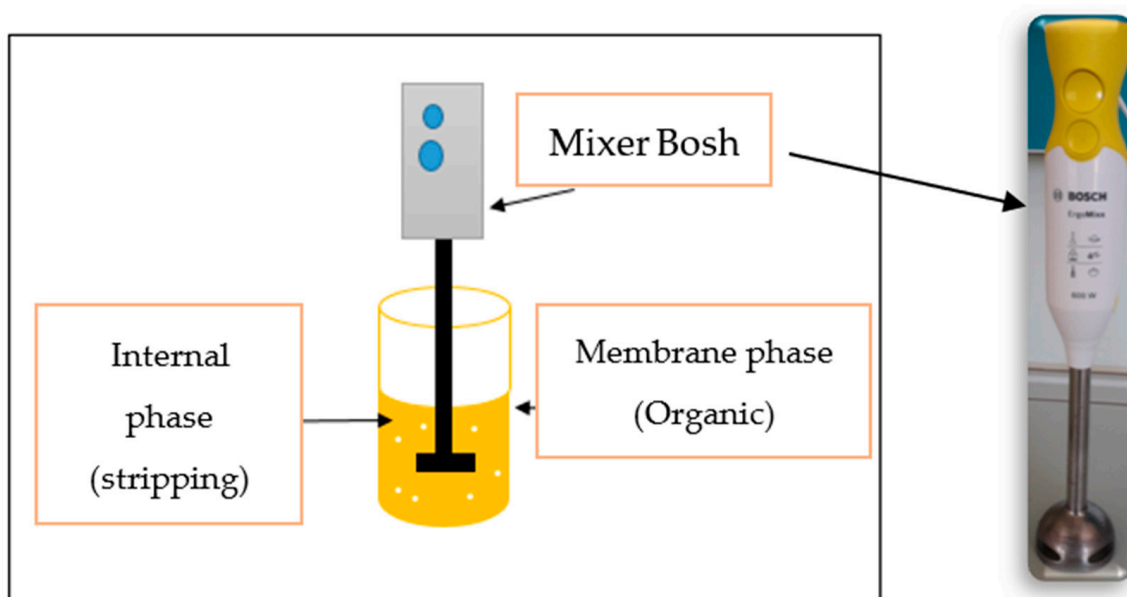


**Figure 1.** Emulsion preparation.

### 2.3. Study of Emulsion Stability

To study the membrane stability, the emulsion prepared previously was combined with 200 mL of distilled water, considered as the external phase (Figure 2). Then, the pH of

the distilled water was monitored for 20 min using a pH meter (HANNA HI 8424, HANNA Instruments, Smithfield, RI, USA). Since the internal phase is acidic, the breakage of the emulsion is detected by decreasing the pH of the external solution [23,54].

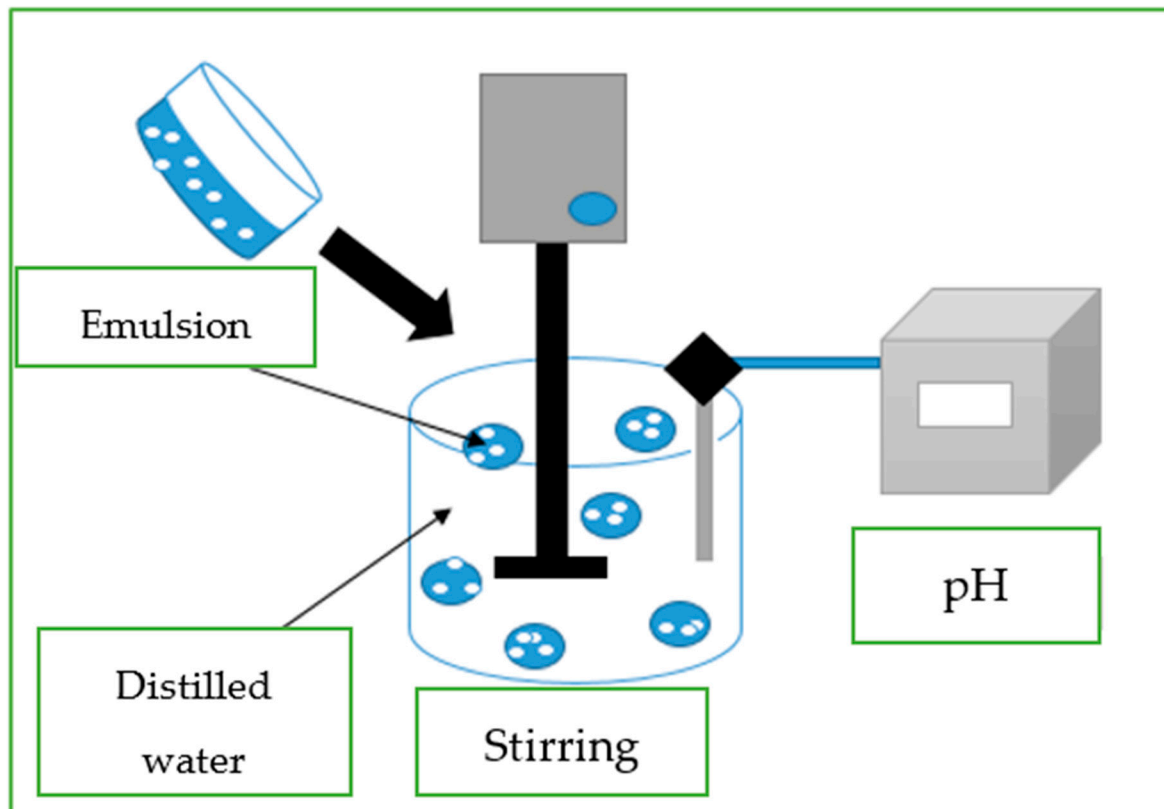


**Figure 2.** Experimental setup for the study of membrane stability.

The membrane rupture rate is defined as follows:

$$T_r = \frac{V_r}{V_i} * 100 \quad (1)$$

with:

$V_r$ : Volume of internal phase leaked into the external phase;

$V_i$ : Initial volume of internal aqueous phase;

The rupture volume ( $V_r$ ) is calculated by mass-balance as follows:

$$V_r = V_{0\text{ext}} \left( \frac{10^{-\text{pH}_0} - 10^{-\text{pH}}}{10^{-\text{pH}} - [\text{H}^+]_i} \right) \quad (2)$$

where:

$V_{0\text{ext}}$ : is the initial external phase volume

$\text{pH}_0$ : initial pH of the external phase

$\text{pH}$ : the pH of the external phase after contact with the emulsion as a function of the time of agitation

$[\text{H}^+]_i$ : the proton's initial concentration in the stripping phase.

The parameters considered for the study of the membrane stability were the concentration of the internal phase solution (nitric acid) [0.2–0.5] M, the percentage of Span 80 [0.5–3]%wt./wt., the emulsification time [1–7] min, the volume ratio of the internal phase to the organic phase (membrane) [1/1–2/1], the volume ratio of the emulsion to the external phase [0.05/1–0.5/1], and the stirring speed [100–600] rpm.

## 2.4. Artificial Neural Network

Artificial neural network (ANN) is a nonlinear empirical model [41]. In general, it is made up of many units (neurons) that work in conjunction. This network's operation is mostly governed by the connections between these elements [42]. Neurons are divided into three different layers: input layer, output layer, and hidden layer [43]. The number of neurons in the input layer corresponds to the number of variables in the input layer, while the number of neurons in the output layer is equal to the number of variables in the output layer [44]. Between these two layers is at least one hidden layer whose number of neurons depends on the network algorithm's application [44].

In this work, ANN was used to predict the volume of the internal phase leaked into the external phase (Y), where parameters: time (X1), acid concentration (X2), surfactant percentage (X3), emulsion time (X4), internal phase to organic phase ratio (X5), emulsion phase to external phase ratio (X6), and stirring speed (X7) were used as inputs.

In order to obtain an optimal result, the architecture of ANN has been optimized [45]. Early on, the back-propagation neural network and the Levenberg Marquardt (LM) learning algorithm were fixed. Then, the database was divided into three: 70% for learning, 15% for testing, and 15% for validation. The number of hidden layer neurons was then optimized with activation functions; they were optimized from 3 to 30. On the other hand, three activation functions were optimized: tansig, logsig, and purelin.

On the other hand, the correlation coefficient (R) and the root mean square error (RMSE) were used to evaluate the efficiency of the model. These two statistical parameters are calculated using the following [46,47]:

$$R = \frac{\sum_{i=1}^N (y_{exp} - \bar{y}_{exp})(y_{pred} - \bar{y}_{pred})}{\sqrt{\sum_{i=1}^N (y_{exp} - \bar{y}_{exp})^2 \sum_{i=1}^N (y_{pred} - \bar{y}_{pred})^2}} \quad (3)$$

$$RMSE = \sqrt{\left(\frac{1}{N}\right) \left(\sum_{i=1}^N [(y_{exp} - \bar{y}_{exp})]^2\right)} \quad (4)$$

where N represents the number of data;  $y_{exp}$  and  $y_{pred}$  are, respectively, the experimental and the predicted values;  $\bar{y}_{exp}$  and  $\bar{y}_{pred}$  are, respectively, the average values of the experimental and the predicted values.

## 3. Results and Discussion

### 3.1. Effect of the Internal Phase Concentration

The concentration and composition of the internal phase have a significant effect on the stability of the membrane and the release of the internal solution to the outside of the emulsion globules. Thus, the effects of the nitric acid solution (HNO<sub>3</sub>) used as the internal phase reagent was studied for concentrations ranging from 0.2 to 2 M; while the percent Span (SP) was 2% wt./wt., the emulsification time was 3 min, hexane was used as a diluent, the ratio of the internal phase volume to the membrane was 1:1, the ratio of the emulsion phase volume to the external phase (distilled water) was 0.15:1, and the stirring speed of the external phase with the emulsion was 250 rpm. The results related to the impact of the internal phase concentration effect are illustrated in Figure 3.

These findings indicate that increasing the concentration of nitric acid in the internal phase from 0.2M to 0.5M increased the stability of the emulsion W/O, hence decreasing the rupture rate from 0.38% to 0.07%. Beyond an HNO<sub>3</sub> concentration of 0.5M, the membrane stability decreased gradually with the increase in nitric acid.

The increase in emulsion breakage is indicative of the gradual release of H<sup>+</sup> cations from the internal phase to the external feed phase (distilled water) with increasing acid concentrations from 1M to 2.5M. This could be attributed to the reaction of the Span 80 with

HNO<sub>3</sub>, leading to the reduction of the surfactant properties and hence the destabilization of the emulsion [53].

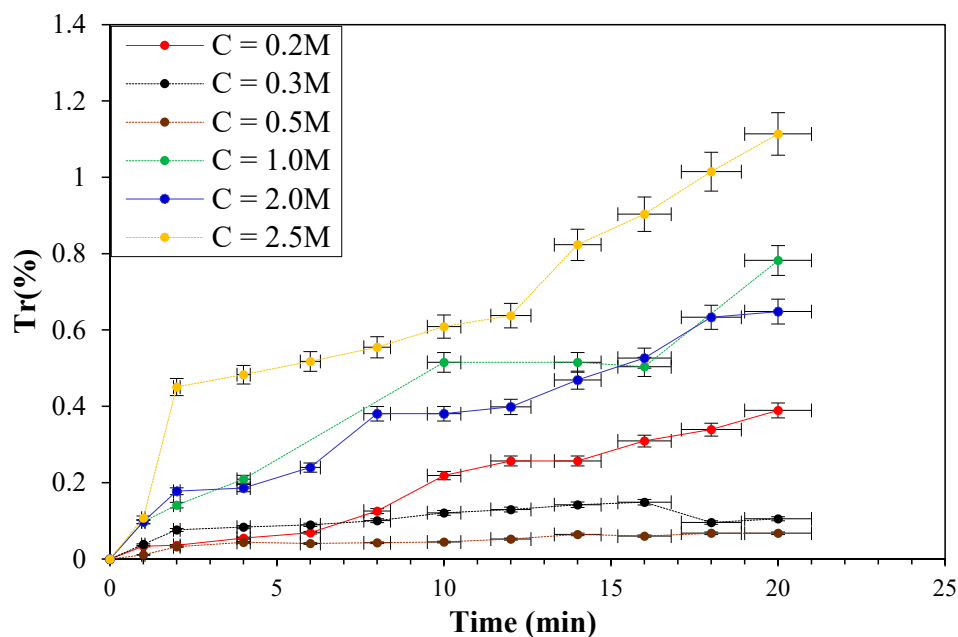


**Figure 3.** Influence of the internal phase concentration on the emulsion stability ([Span 80]: 2% wt./wt., w: 250 rpm, int/org (v/v): 1/1, emu/ext (v/v): 0.15/1,  $t_{\text{emuls}} = 3$  min, internal phase: HNO<sub>3</sub>).

Thus, the nitric acid concentration for which the lowest breaking rate (0.07%) was obtained was 0.5 M; this acid concentration provided very high emulsion stability.

### 3.2. Effect of the Surfactant Concentration

The effect of the surfactant (Span 80) concentration on the emulsion stability was studied by varying the surfactant concentration in the range of 0.5 to 3%wt./wt. The results obtained (Figure 4) show that the increase in surfactant concentration caused a decrease in the rupture rate (Tr%) up to 2% wt./wt., where we observed a destabilization of the membrane.

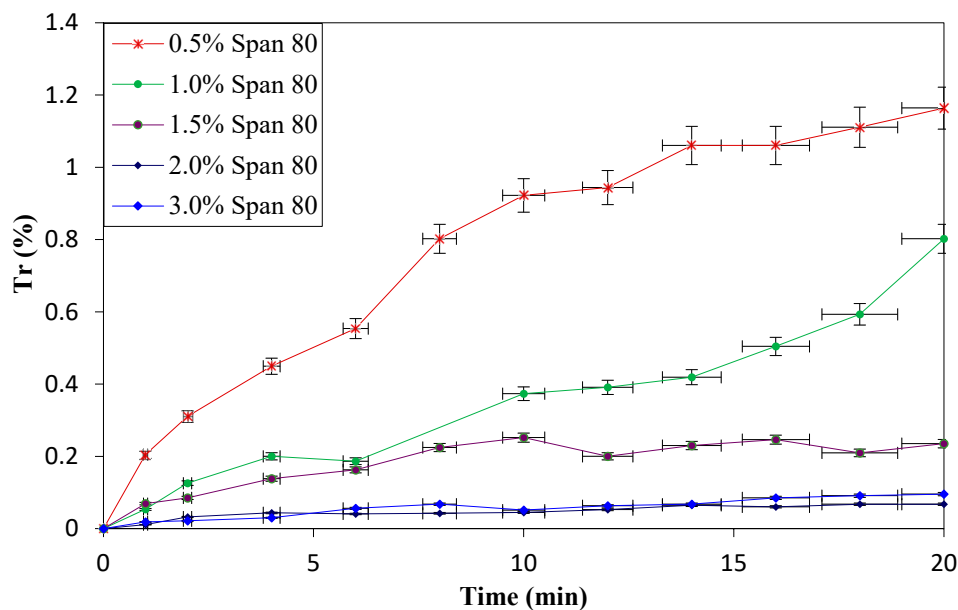


**Figure 4.** Effect of the Span 80 concentration on the emulsion stability ([Span 80]: [0.5–2] % wt./wt., w: 250 rpm, int/org (v/v): 1/1, emu/ext (v/v): 0.15/1,  $t_{\text{emuls}} = 3$  min, [HNO<sub>3</sub>Internal phase]: 0.5M).

The surfactant acts as a protective barrier between the external and aqueous internal phases in the ELM process by producing a thin layer at the interface of the two phases, which prevents water leakage, the swelling of emulsion globules, and the breaking of the emulsion [55,56].

For low surfactant concentrations (<2% wt./wt.), the barrier formed at the water-oil interface is too weak, which makes the emulsion brittle and breaks easily, as the amount of surfactant present in the organic phase is insufficient to surround the entire internal water phase [55,56]. With a low amount of tension active, the interfacial tension is important [3]. Hence, the emulsion droplets tend to collide and coalesce with each other during emulsification to form larger emulsion globules providing a weaker interfacial area for mass transfer and leading to the melting of the inner phase droplets into the membrane phase and the inability to protect the emulsion breakage [56,57].

Above the optimal Span 80 concentration of 2% wt./wt., a decrease in emulsion stability is produced; the addition of a high surfactant quantity promotes the aggregation of the surfactant in the bulk solution. The defensive barrier becomes useless with the addition of more surfactant; the aggregates produced favor the transfer of water from the internal phase to the external phase, which leads to the rupture, and the swelling of the membrane [3,58]. Therefore, 2% wt./wt. of Span 80 was selected as the optimum surfactant concentration with low breakage of 0.07%.

### 3.3. Effect of the Emulsification Time

One of the most important parameters for the ELM process is the emulsification time. To study its effect, the membrane stability test was conducted for a surfactant concentration of 2% (wt./wt.), an internal phase concentration ( $\text{HNO}_3$ ) of 0.5 M, distilled water as the external phase, volume ratios of internal phase to organic phase of 1:1 and emulsion to the external phase of 0.15:1 (Figure 5).

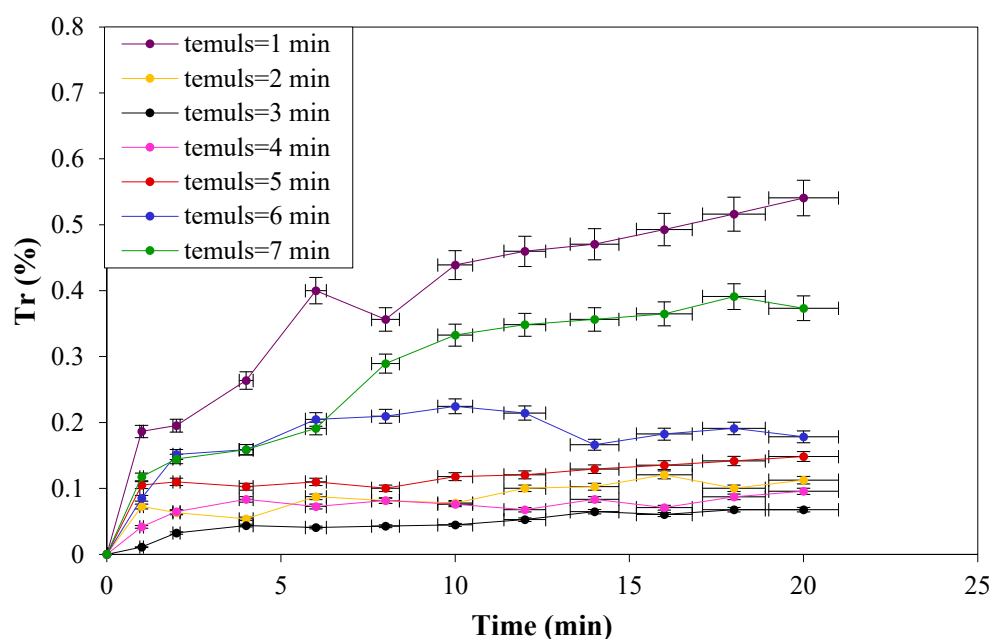


**Figure 5.** Effect of the emulsification time on emulsion stability (C Span 80: 2% wt./wt.,  $w$ : 250 rpm, int/org ( $v/v$ ): 1/1, emu/ext ( $v/v$ ): 0.15/1,  $t_{\text{emuls}} = [1-7]$  min,  $[\text{HNO}_3]_{\text{Internal phase}} = 0.5\text{M}$ ).

Due to a lack of homogeneity between the membrane and the internal phase, the production of large-sized droplets led to the coalescence and loss of stability of the organic phase for an inadequate emulsification duration of 1 min (0.54%) [17,56].

For a very long emulsification time (5, 6, and 7 min), the breakage of the organic phase was also high since the breakage of the internal phase led to a large number of small



droplets per unit volume. The distance between them decreases significantly, facilitating their coalescence and subsequent expulsion from the internal to the external aqueous phase. On the other hand, a long duration of agitation increases the internal shearing rate, also causing the formation of a high number of small emulsion globules per unit of volume and leading to a decrease in the viscoelastic characteristics of the emulsion and, thus, a thinner organic membrane layer [17,57,59].

The breakage rate started to decrease with increasing emulsification time from 2 to 3 min, but the lowest breakage rate was recorded at 3 min; this emulsification time offers excellent emulsion stability, which implies that the steady state has been reached, thus an emulsification time of 3 min was chosen as optimal for further work.

### 3.4. Effect of the Volume Ratio of Internal to Organic Phase

To investigate the impact of the Volume ratio internal phase to organic phase ( $V_{\text{Internal phase}}/V_{\text{Organic phase}}$ ) on emulsion stability and membrane rupture, the volume ratio of internal phase to organic phase was varied as follows 1:2, 1:4, 3:2, 2:1.

As shown in Figure 6, at a low phase ratio, the rupture rate registered was 0.25%; by increasing the phase ratio to 3/4, the rupture rate reached the lowest value of 0.07%. However, increasing the phase ratio beyond the optimum value of 3/4 led to an increase in the membrane rupture rate from 0.07% to 1.65% for a phase ratio of 2/1.

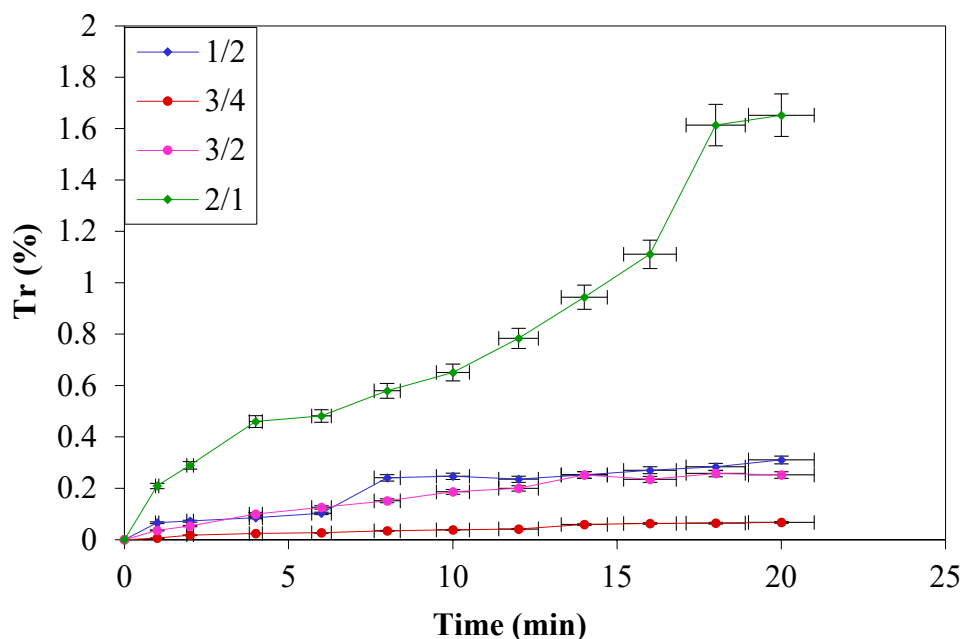


**Figure 6.** Effect of the volume ratio of internal phase to organic phase (CSpan 80: 2% wt./wt., w: 250 rpm, int/org ( $v/v$ ): [1/1–2/1], emu/ext ( $v/v$ ): 0.15/1,  $t_{\text{emuls}} = 3$  min,  $[\text{HNO}_3]_{\text{Internal phase}} = 0.5\text{M}$ ).

For the volume ratio (1/2), the additional organic content raises the membrane's viscosity and thickness due to high organic content, thus leading to an increase in the size of the globules of the emulsion and consequently reducing the interfacial area between the external phase and the emulsion. In other terms, the surfactant amount in this film probably becomes insufficient to hold longer [3,60].

For volumetric ratios of 2/1 and 3/2, when the volume of the internal phase is greater than that of the membrane phase, the breakup is significant. This leads to a shift of internal droplet size distribution to larger sizes and increases the viscosity of the emulsion. In addition, the volume of the organic phase for both ratios becomes insufficient to contain the entire internal aqueous phase, making it difficult to disperse the W/O emulsion [3,56,61,62].

In this study, a volume ratio of 3/4 between the internal aqueous phase and the membrane phase was therefore deemed appropriate.

### 3.5. Effect of the Volume Ratio of the Emulsion Phase to the External Phase

The emulsion-to-external-solution volume ratio governs the interfacial mass transfer across ELMs. It is the same as the ratio of solvent to feed in conventional liquid extraction [53,56]. To examine this effect, the volume ratio of the emulsion phase to the external phase varied from 0.05/1 to 0.5/1 (Figure 7).

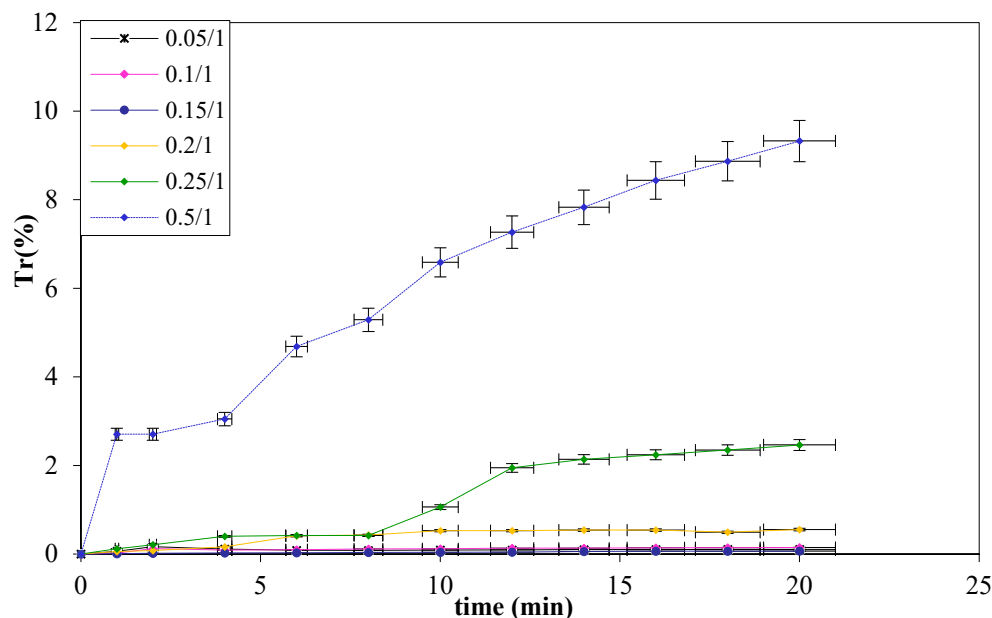


**Figure 7.** Effect of the ratio of emulsion phase to external phase on emulsion stability (Cspan 80: 2% wt./wt., w: 250 rpm, int/org (v/v): (3/4), emu/ext (v/v): [0.05/1–0.5/1],  $t_{\text{emuls}} = 3$  min,  $[\text{HNO}_3]_{\text{Internal phase}} = 0.5\text{M}$ ).

The influence of the volume ratio of the external phase to the membrane phase W/O was not significant for volume ratio values of 0.05 to 0.15%, owing to the slight increase in the rupture with the increase in this volume ratio.

By increasing the volume ratio beyond 0.15, the rupture rate increased gradually until reaching 9.22% for a volume ratio of 0.5%; this is a consequence of the increase in the coalescence of the internal droplets giving embrittlement and rupture of the membrane [53].

These results led to deduce that it is necessary to respect a certain proportionality between the volume of the emulsion and the external phase [63]; thus, the volume ratio of 0.15/1 was chosen as the optimal volume ratio.

### 3.6. Effect of the Stirring Speed

The effect of stirring speed (100–600) rpm on the stability of the emulsion W/O is shown in Figure 8.

The obtained results (Figure 8) show that the breakage rate was not greatly affected by increasing the stirring speed from 100 to 250 rpm; suitable stability with a very low rupture rate (0.07%) of the W/O emulsions was obtained for the agitation speed of 250 rpm. This is due to the decrease in emulsion globule size and the increase in interfacial area for mass transfer when the agitation level is increased to 250 rpm [17,53].

By raising the stirring speed over a threshold value of 250 rpm, the emulsion's stability was compromised. This is because the fast stirring speed increases the dispersion of emulsion globules in the treated phase, where a large interfacial area of material transfer is achieved by the production of tiny globules, favoring ejection from the internal phase to the external phase. When the agitation speed is lower than 250 rpm, the emulsion globule size increases, and the interfacial area accessible for mass transfer diminishes. In other words, emulsion dissolution is more intense, and internal phase leakage occurs. This may be explained by the membrane's enhanced osmotic swelling [8].

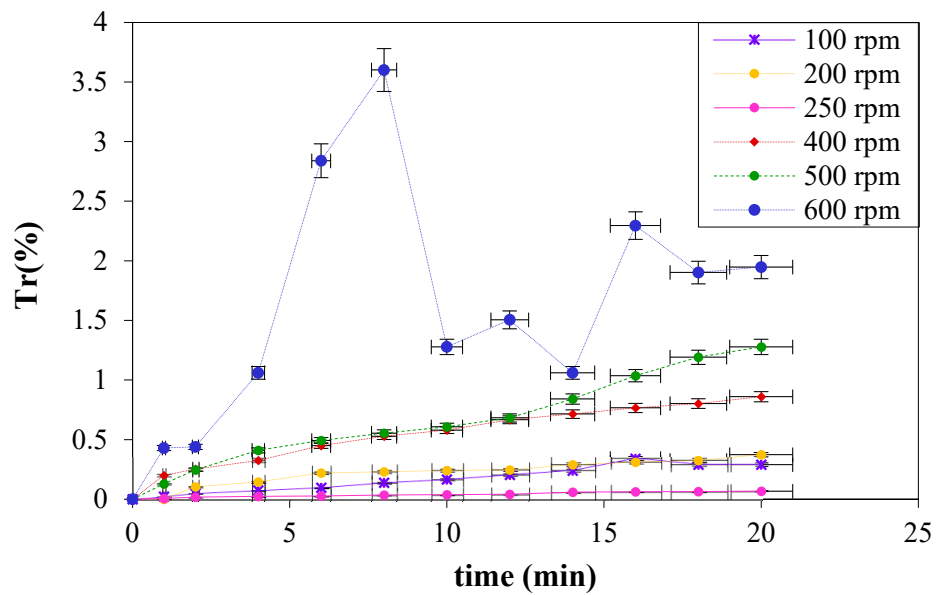


**Figure 8.** Effect of the stirring speed on the emulsion stability (C Span 80: 2% wt./wt., w: (100–600) rpm, int/org (v/v): (3/4), emu/ext (v/v): 0.15/1,  $t_{emuls} = 3$  min,  $[HNO_3]_{Internal\ phase} : 0.5M$ ).

Therefore, a stirring speed of 250 rpm should be performed to ensure suitable stability of W/O emulsions and to improve the interfacial area available for mass transfer.

### 3.7. Artificial Neural Network

As discussed earlier, the development of ANN was based on optimizing the number of hidden layer neurons and activation functions.

The optimization results show that the best result was obtained at the architecture [7–9–1] with the function tansig at the hidden layer and purelin at the output (Figure 9); the optimal results depending on R and RMSE of each phase are presented in Table 1.

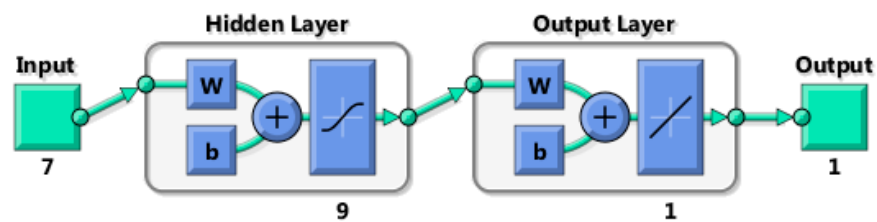


**Figure 9.** Schematic representation of the ANN model.

**Table 1.** Performances of the ANN architecture.

Network architecture	Activation Function		Coefficients of Determination				RMSE			
	Hidden layer	Output layer	Training	Validation	Test	ALL	Training	Validation	Test	ALL
[7–9–1]	tansig	purelin	0.99724	0.99802	0.99852	0.99772	0.0378	0.0420	0.0509	0.0406

Table 1 displays the best architectures observed. It presents the correlation coefficients and errors for each training, test, and validation based on the number of neurons in the hidden layer and the topology of the network. In addition, the activation functions for the hidden layer and output layer are shown. From Table 1, the correlation coefficients of the training, validation, test, and all data phase were almost 1 ( $R_{training} = 0.99724$ ;  $R_{validation} = 0.99802$ ;  $R_{test} = 0.99852$ ;  $R_{all\ data} = 0.99772$ ), and also the statistical errors of RMSE in the four phases were almost 0 ( $RMSE_{training} = 0.0378$ ;

RMSE\_validation = 0.0420; RMSE\_test = 0.0509; RMSE\_all data = 0.0406). This shows the efficiency of the model obtained.

Additionally, these results have been presented graphically in Figure 10.

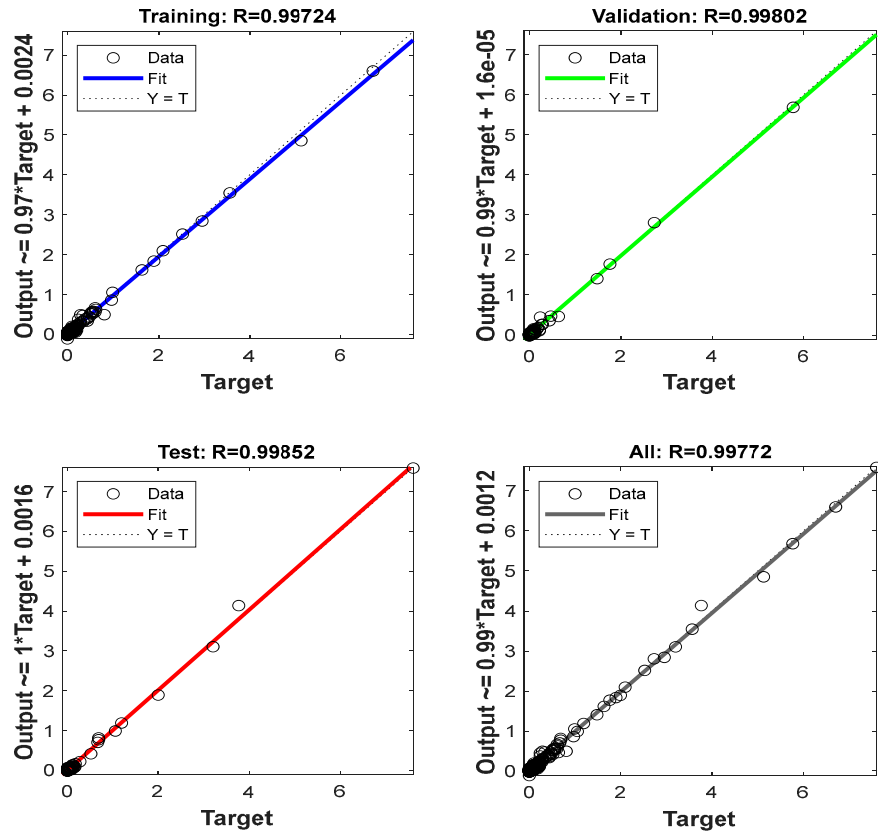


Figure 10. Relationship between experimental values and values predicted by the ANN model.

To confirm the performance of this model, analysis of the residue was launched by the frequency method (Figure 11a) and also by the histogram of error method (Figure 11b).

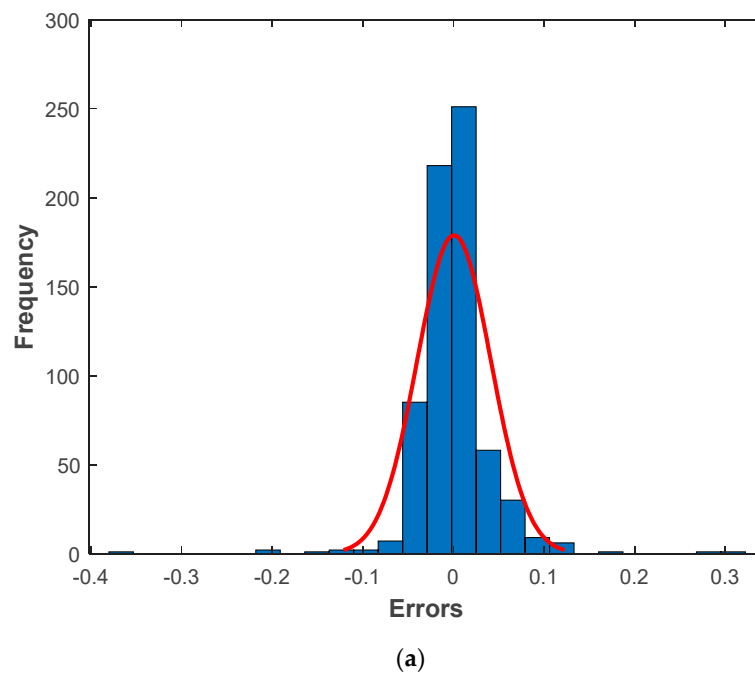
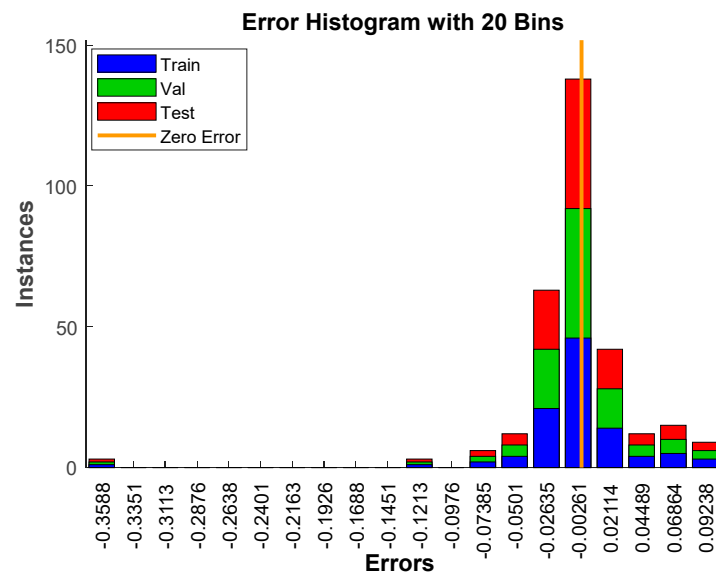


Figure 11. Cont.



(b)

**Figure 11.** Residuals relating to the model established by the different techniques according to the estimated values: (a) frequency distribution of errors, and (b) histogram of error values with 20 bins.

The figure showed that the optimal frequency was obtained in error 0. In addition, the figure also showed that the errors that were recorded are in the interval  $[-1,1]$ . It was confirmed by the histogram of the error method because the errors recorded for the three phases (training, testing, and validation) were all above 0.

From these arguments, it is obvious that the ANN model is effective.

#### 4. Conclusions

The purpose of this study was to set the optimal conditions for maintaining a stable emulsion; the result of optimization revealed that the stability of the emulsion depends on several conditions. The concentration of the surfactant, the emulsification duration, and the stirring speed were found to be crucial elements that contribute to membrane breakage. Using a concentration of nitric acid equal to 0.5 M as the internal phase, 2% wt./wt. of Span 80 as a surfactant, a 3 min emulsification time, volume ratios of 3/4 and 0.15/1 for (Internal/organic phase) and (emulsion/external), respectively, and a stirring speed of 250 rpm a suitable membrane stability was obtained with a decreasing rupture rate ( $Tr$ ) until reaching a minimum value of 0.07%. Since the stability of emulsions is one of the major obstacles in the industrial use of ELM, these results provide a suitable indication of the suitability of its application.

On the other hand, the ANN model demonstrated extremely high accuracy due to the very high statistical coefficients in the four phases ( $R_{\text{training}} = 0.99724$ ;  $R_{\text{validation}} = 0.99802$ ;  $R_{\text{test}} = 0.99852$ ;  $R_{\text{all data}} = 0.99772$ ), and very low statistical errors of RMSE in the four phases ( $RMSE_{\text{training}} = 0.0378$ ;  $RMSE_{\text{validation}} = 0.0420$ ;  $RMSE_{\text{test}} = 0.0509$ ;  $RMSE_{\text{all data}} = 0.0406$ ). Moreover, the efficiency of the model was proven by the residual analyses, showing the relevance of the ANN model.

**Author Contributions:** Conceptualization, M.Z., Z.L. and L.M.; methodology, M.Z., H.T. and L.M.; validation, A.A., S.M., R.C. and L.M.; formal analysis, H.T., M.I.K. and M.Z.; investigation, A.H.; resources, L.M. and A.A.; data curation, M.Z., H.T. and S.M.; writing—original draft preparation, M.Z.; writing—review and editing, A.H., A.A., L.M., H.T. and M.I.K.; visualization, Z.L., L.M., M.I.K. and A.A.; supervision, L.M. and A.A.; project administration, L.M. and A.A. All authors have read and agreed to the published version of the manuscript.

**Funding:** This research received no external funding.

**Institutional Review Board Statement:** Not applicable.

**Informed Consent Statement:** Not applicable.

**Data Availability Statement:** Not applicable.

**Acknowledgments:** The authors wish to thank all who assisted in conducting this work.

**Conflicts of Interest:** The authors declare no conflict of interest.

## References

1. Kargari, A.; Kaghazchi, T.; Soleimani, M. Role of emulsifier in the extraction of gold (III) ions from aqueous solutions using the emulsion liquid membrane technique. *Desalination* **2004**, *162*, 237–247. [[CrossRef](#)]
2. He, K.; Tang, J.; Weng, H.; Chen, G.; Wu, Z.; Lin, M. Efficient extraction of precious metal ions by a membrane emulsification circulation extractor. *Sep. Purif. Technol.* **2019**, *213*, 93–100. [[CrossRef](#)]
3. Ting, H.C.; Khan, H.W.; Reddy, A.V.B.; Goto, M.; Moniruzzaman, M. Extraction of salicylic acid from wastewater using ionic liquid-based green emulsion liquid membrane: COSMO-RS prediction and experimental verification. *J. Mol. Liq.* **2022**, *347*, 118280. [[CrossRef](#)]
4. Zhang, K.; Liang, H.; Zhong, X.; Cao, H.; Wang, R.; Liu, Z. Recovery of metals from sulfate leach solutions of spent ternary lithium-ion batteries by precipitation with phosphate and solvent extraction with P507. *Hydrometallurgy* **2022**, *210*, 105861. [[CrossRef](#)]
5. Sole, K.C.; Hiskey, J.B. Solvent extraction characteristics of thiosubstituted organophosphinic acid extractants. *Hydrometallurgy* **1992**, *30*, 345–365. [[CrossRef](#)]
6. Wang, Y.G.; Yue, S.T.; Li, D.Q.; Jin, M.J.; Li, C.Z. Solvent Extraction of Scandium(III), Yttrium(III), Lanthanides(III), and divalent metal ions with sec-nonylphenoxy acetic acid. *Solvent Extr. Ion Exch.* **2002**, *20*, 701–716. [[CrossRef](#)]
7. Xing, W.D.; Lee, M.S.; Senanayake, G. Recovery of metals from chloride leach solutions of anode slimes by solvent extraction. Part I: Recovery of gold with Cyanex 272. *Hydrometallurgy* **2018**, *180*, 58–64. [[CrossRef](#)]
8. Ye, Q.; Li, G.; Deng, B.; Luo, J.; Rao, M.; Peng, Z.; Zhang, Y.; Jiang, T. Solvent extraction behavior of metal ions and selective separation Sc<sup>3+</sup> in phosphoric acid medium using P204. *Sep. Purif. Technol.* **2019**, *209*, 175–181. [[CrossRef](#)]
9. Zhu, K.; Wei, Q.; Li, H.; Ren, X. Solvent extraction of titanium from ilmenite hydrochloric acid leachate: Optimization and investigation of extraction reactions of all contained metal ions. *Miner. Eng.* **2022**, *186*, 107744. [[CrossRef](#)]
10. Asrami, M.R.; Tran, N.N.; Nigam, K.D.P.; Hessel, V. Solvent extraction of metals: Role of ionic liquids and microfluidics. *Sep. Purif. Technol.* **2021**, *262*, 118289. [[CrossRef](#)]
11. Pavón, S.; Haneklaus, N.; Meerbach, K.; Bertau, M. Iron(III) removal and rare earth element recovery from a synthetic wet phosphoric acid solution using solvent extraction. *Miner. Eng.* **2022**, *182*, 107569. [[CrossRef](#)]
12. León, G.; Gómez, E.; Miguel, B.; Hidalgo, A.M.; Gómez, M.; Murcia, M.D.; Guzmán, M.A. Feasibility of Adsorption Kinetic Models to Study Carrier-Mediated Transport of Heavy Metal Ions in Emulsion Liquid Membranes. *Membranes* **2022**, *12*, 66. [[CrossRef](#)] [[PubMed](#)]
13. León, L.; León, G.; Senent, J.; Pérez-Sirvent, C. Optimization of Copper Removal from Aqueous Solutions Using Emulsion Liquid Membranes with Benzoylacetone as a Carrier. *Metals* **2017**, *7*, 19. [[CrossRef](#)]
14. Ferreira, L.C.; Ferreira, L.C.; Cardoso, V.L.; Filho, U.C. Mn(II) removal from water using emulsion liquid membrane composed of chelating agents and biosurfactant produced in loco. *J. Water Process Eng.* **2019**, *29*, 100792. [[CrossRef](#)]
15. Sujatha, S.; Rajasimman, M. Development of a green emulsion liquid membrane using waste cooking oil as diluent for the extraction of arsenic from aqueous solution—Screening, optimization, kinetics and thermodynamics studies. *J. Water Process Eng.* **2021**, *41*, 102055.
16. Liu, H.; Zhang, Y.; Huang, J.; Liu, T.; Xue, N.; Wang, K. Selective separation and recovery of vanadium from a multiple impurity acid leaching solution of stone coal by emulsion liquid membrane using di-(2-ethylhexyl)phosphoric acid. *Chem. Eng. Res. Des.* **2017**, *122*, 289–297. [[CrossRef](#)]
17. Sulaiman, R.N.R.; Othman, N.; Amin, N.A.S. Emulsion liquid membrane stability in the extraction of ionized nanosilver from wash water. *J. Ind. Eng. Chem.* **2014**, *20*, 3243–3250. [[CrossRef](#)]
18. Kiani, S.; Mousavi, S.M. Ultrasound assisted preparation of water in oil emulsions and their application in arsenic (V) removal from water in an emulsion liquid membrane process. *Ultrason. Sonochem.* **2013**, *20*, 373–377. [[CrossRef](#)]
19. Klemz, A.C.; Weschenfelder, S.E.; de Carvalho Neto, S.L.; Damas, M.S.P.; Viviani, J.C.T.; Mazur, L.P.; Marinho, B.A.; Pereira, L.D.S.; da Silva, A.; Borges Valle, J.A.; et al. Oilfield produced water treatment by liquid-liquid extraction: A review. *J. Pet. Sci. Eng.* **2021**, *199*, 108282. [[CrossRef](#)]
20. Mohammed, A.A.; Atiya, M.A.; Hussein, M.A. Studies on membrane stability and extraction of ciprofloxacin from aqueous solution using pickering emulsion liquid membrane stabilized by magnetic nano-Fe<sub>2</sub>O<sub>3</sub>. *Colloids Surf. A Physicochem. Eng. Asp.* **2020**, *585*, 124044. [[CrossRef](#)]

21. Alitabar-Ferozjah, H.; Rahbar-Kelishami, A. Simultaneous effect of multi-walled carbon nanotube and Span85 on the extraction of Ibuprofen from aqueous solution using emulsion liquid membrane. *J. Mol. Liq.* **2022**, *365*, 120051. [[CrossRef](#)]
22. Al-Obaidi, Q.; Alabdulmuhsin, M.; Tolstik, A.; Trautman, J.G.; Al-Dahhan, M. Removal of hydrocarbons of 4-Nitrophenol by emulsion liquid membrane (ELM) using magnetic Fe<sub>2</sub>O<sub>3</sub> nanoparticles and ionic liquid. *J. Water Process Eng.* **2021**, *39*, 101729. [[CrossRef](#)]
23. Salman, H.M.; Mohammed, A.A. Extraction of lead ions from aqueous solution by co-stabilization mechanisms of magnetic Fe<sub>2</sub>O<sub>3</sub> particles and nonionic surfactants in emulsion liquid membrane. *Colloids Surf. A Physicochem. Eng. Asp.* **2019**, *568*, 301–310. [[CrossRef](#)]
24. Qian, H.; Yang, Q.; Qu, Y.; Ju, Z.; Zhou, W.; Gao, H. Hydrophobic deep eutectic solvents based membrane emulsification-assisted liquid-phase microextraction method for determination of pyrethroids in tea beverages. *J. Chromatogr. A* **2020**, *1623*, 461204. [[CrossRef](#)] [[PubMed](#)]
25. Correia, P.F.M.M.; de Carvalho, J.M.R. Recovery of phenol from phenolic resin plant effluents by emulsion liquid membranes. *J. Membr. Sci.* **2003**, *225*, 41–49. [[CrossRef](#)]
26. Bahloul, L.; Ismail, F.; Samar, M.E.-H.; Meradi, H. Removal of AY99 from an Aqueous Solution Using an Emulsified Liquid Membrane. Application of Plackett-burman Design. *Energy Procedia* **2014**, *50*, 1008–1016. [[CrossRef](#)]
27. Eyupoglu, V.; Kumbasar, R.A. Extraction of Ni(II) from spent Cr–Ni electroplating bath solutions using LIX 63 and 2BDA as carriers by emulsion liquid membrane technique. *J. Ind. Eng. Chem.* **2015**, *21*, 303–310. [[CrossRef](#)]
28. Zhu, G.; Wang, Y.; Huang, Q.; Zhang, R.; Chen, D.; Wang, S.; Yang, X. Emulsion liquid membrane for simultaneous extraction and separation of copper from nickel in ammoniacal solutions. *Miner. Eng.* **2022**, *188*, 107849. [[CrossRef](#)]
29. Okamoto, Y.; Nomura, Y.; Nakamura, H.; Iwamaru, K.; Fujiwara, T.; Kumamaru, T. High preconcentration of ultra-trace metal ions by liquid–liquid extraction using water/oil/water emulsions as liquid surfactant membranes. *Microchem. J.* **2000**, *65*, 341–346. [[CrossRef](#)]
30. Kumbasar, R.A. Selective extraction and concentration of chromium(VI) from acidic solutions containing various metal ions through emulsion liquid membranes using Amberlite LA-2. *J. Ind. Eng. Chem.* **2010**, *16*, 829–836. [[CrossRef](#)]
31. Uddin, M.S.; Kathiresan, M. Extraction of metal ions by emulsion liquid membrane using bi-functional surfactant: Equilibrium and kinetic studies. *Sep. Purif. Technol.* **2000**, *19*, 3–9. [[CrossRef](#)]
32. Zhang, L.; Chen, Q.; Kang, C.; Ma, X.; Yang, Z. Rare earth extraction from wet process phosphoric acid by emulsion liquid membrane. *J. Rare Earths* **2016**, *34*, 717–723. [[CrossRef](#)]
33. Chen, Q.; Ma, X.; Zhang, X.; Liu, Y.; Yu, M. Extraction of rare earth ions from phosphate leach solution using emulsion liquid membrane in concentrated nitric acid medium. *J. Rare Earths* **2018**, *36*, 1190–1197. [[CrossRef](#)]
34. Kumbasar, R.A.; Tutkun, O. Separation and concentration of gallium from acidic leach solutions containing various metal ions by emulsion type of liquid membranes using TOPO as mobile carrier. *Hydrometallurgy* **2004**, *75*, 111–121. [[CrossRef](#)]
35. Anarakdim, K.; Matos, M.; Cambiella, A.; Senhadji-Kebiche, O.; Gutiérrez, G. Effect of temperature on the heat treatment to recover green solvent from emulsion liquid membranes used in the extraction of Cr(VI). *Chem. Eng. Process.—Process Intensif.* **2020**, *158*, 108178. [[CrossRef](#)]
36. Kankekar, P.S.; Wagh, S.J.; Mahajani, V.V. Process intensification in extraction by liquid emulsion membrane (LEM) process: A case study; enrichment of ruthenium from lean aqueous solution. *Chem. Eng. Process. Process Intensif.* **2010**, *49*, 441–448. [[CrossRef](#)]
37. Asadian, H.; Ahmadi, A. The extraction of gallium from chloride solutions by emulsion liquid membrane: Optimization through response surface methodology. *Miner. Eng.* **2020**, *148*, 106207. [[CrossRef](#)]
38. Abbassian, K.; Kargari, A. Modification of membrane formulation for stabilization of emulsion liquid membrane for extraction of phenol from aqueous solutions. *J. Environ. Chem. Eng.* **2016**, *4*, 3926–3933. [[CrossRef](#)]
39. Correia, P.F.M.M.; Carvalho, J.M.R.D. Recovery of 2-chlorophenol from aqueous solutions by emulsion liquid membranes: Batch experimental studies and modelling. *J. Membr. Sci.* **2000**, *179*, 175–183. [[CrossRef](#)]
40. Correia, P.F.M.M.; de Carvalho, J.M.R. A comparison of models for 2-chlorophenol recovery from aqueous solutions by emulsion liquid membranes. *Chem. Eng. Sci.* **2001**, *56*, 5317–5325. [[CrossRef](#)]
41. Bahloul, L.; Bendebane, F.; Djenouhat, M.; Meradi, H.; Ismail, F. Effects and optimization of operating parameters of anionic dye extraction from an aqueous solution using an emulsified liquid membrane: Application of designs of experiments. *J. Taiwan Inst. Chem. Eng.* **2016**, *59*, 26–32. [[CrossRef](#)]
42. Bahloul, L.; Ismail, F.; Samar, M.E.-H. Extraction and Desextraction of a Cationic Dye using an Emulsified Liquid Membrane in an Aqueous Solution. *Energy Procedia* **2013**, *36*, 1232–1240. [[CrossRef](#)]
43. Rosly, M.B.; Jusoh, N.; Othman, N.; Rahman, H.A.; Noah, N.F.M.; Sulaiman, R.N.R. Synergism of Aliquat336-D2EHPA as carrier on the selectivity of organic compound dyes extraction via emulsion liquid membrane process. *Sep. Purif. Technol.* **2020**, *239*, 116527. [[CrossRef](#)]
44. Zereshki, S.; Daraei, P.; Shokri, A. Application of edible paraffin oil for cationic dye removal from water using emulsion liquid membrane. *J. Hazard. Mater.* **2018**, *356*, 1–8. [[CrossRef](#)] [[PubMed](#)]
45. Othman, N.; Zailani, S.N.; Mili, N. Recovery of synthetic dye from simulated wastewater using emulsion liquid membrane process containing tri-dodecyl amine as a mobile carrier. *J. Hazard. Mater.* **2011**, *198*, 103–112. [[CrossRef](#)]
46. Das, C.; Rungta, M.; Arya, G.; DasGupta, S.; De, S. Removal of dyes and their mixtures from aqueous solution using liquid emulsion membrane. *J. Hazard. Mater.* **2008**, *159*, 365–371. [[CrossRef](#)] [[PubMed](#)]

47. Seifollahi, Z.; Rahbar-Kelishami, A. Diclofenac extraction from aqueous solution by an emulsion liquid membrane: Parameter study and optimization using the response surface methodology. *J. Mol. Liq.* **2017**, *231*, 1–10. [[CrossRef](#)]
48. Yan, B.; Huang, X.; Chen, K.; Liu, H.; Wei, S.; Wu, Y.; Wang, L. A study of synergetic carrier emulsion liquid membrane for the extraction of amoxicillin from aqueous phase using response surface methodology. *J. Ind. Eng. Chem.* **2021**, *100*, 63–74. [[CrossRef](#)]
49. Jiao, H.; Peng, W.; Zhao, J.; Xu, C. Extraction performance of bisphenol A from aqueous solutions by emulsion liquid membrane using response surface methodology. *Desalination* **2013**, *313*, 36–43. [[CrossRef](#)]
50. Razo-Lazcano, T.A.; del Pilar González-Muñoz, M.; Stambouli, M.; Pareau, D.; Hernández-Perales, L.; Avila-Rodriguez, M. Chlorpheniramine recovery from aqueous solutions by emulsion liquid membranes using soy lecithin as carrier. *Colloids Surf. A Physicochem. Eng. Asp.* **2018**, *536*, 68–73. [[CrossRef](#)]
51. Karmakar, R.; Singh, P.; Datta, A.; Sen, K. Emulsion Liquid Membrane in the Selective Extraction of Dy. *Chem. Eng. Res. Des.* **2022**, *187*, 497–506. [[CrossRef](#)]
52. De Souza, F.B.; de Souza, A.A.U.; Oliveira, J.V.; Ulson, S.M.D.A.G. Green extraction based on emulsion liquid membranes: Removal of Cr (III) from synthetic effluents, Environmental Nanotechnology. *Monit. Manag.* **2021**, *16*, 100579.
53. Mohammed, A.A.; Atiya, M.A.; Hussein, M.A. Simultaneous studies of emulsion stability and extraction capacity for the removal of tetracycline from aqueous solution by liquid surfactant membrane. *Chem. Eng. Res. Des.* **2020**, *159*, 225–235. [[CrossRef](#)]
54. Aouad, A.A.; Bouranene, S.; Gouassmia, A.; Djaber, S.; Zeghadnia, L.; Guebail, A. Study of The Stability of Water-In-Oil Emulsion Intended for the Extraction of Heavy Metals Application: Copper Ions. *Jordanian J. Eng. Chem. Ind. JJEI* **2021**, *4*, 62–69.
55. Raval, A.R.; Kohli, H.P.; Mahadwad, O.K. Application of emulsion liquid membrane for removal of malachite green dye from aqueous solution: Extraction and stability studies. *Chem. Eng. J. Adv.* **2022**, *12*, 100398. [[CrossRef](#)]
56. Dâas, A.; Hamdaoui, O. Extraction of anionic dye from aqueous solutions by emulsion liquid membrane. *J. Hazard. Mater.* **2010**, *178*, 973–981. [[CrossRef](#)]
57. Rosly, M.B.; Jusoh, N.; Othman, N.; Rahman, H.A.; Sulaiman, R.N.R.; Noah, N.F.M. Stability of emulsion liquid membrane using bifunctional diluent and blended nonionic surfactant for phenol removal. *Chem. Eng. Process.—Process Intensif.* **2020**, *148*, 107790. [[CrossRef](#)]
58. Ahmad, A.L.; Kusumastuti, A.; Derek, C.J.C.; Ooi, B.S. Emulsion liquid membrane for cadmium removal: Studies on emulsion diameter and stability. *Desalination* **2012**, *287*, 30–34. [[CrossRef](#)]
59. Purtika; Thakur, A.; Jawa, G.K. Comparative study on effect of ionic liquids on static stability of green emulsion liquid membrane. *Colloids Surf. A Physicochem. Eng. Asp.* **2022**, *644*, 128776. [[CrossRef](#)]
60. Sabry, R.; Hafez, A.; Khedr, M.; El-Hassanin, A. Removal of lead by an emulsion liquid membrane: Part I. *Desalination* **2007**, *212*, 165–175. [[CrossRef](#)]
61. Juang, R.-S.; Lin, K.-H. Ultrasound-assisted production of W/O emulsions in liquid surfactant membrane processes. *Colloids Surf. A Physicochem. Eng. Asp.* **2004**, *238*, 43–49. [[CrossRef](#)]
62. Djenouhat, M.; Hamdaoui, O.; Chiha, M.; Samar, M.H. Ultrasonication-assisted preparation of water-in-oil emulsions and application to the removal of cationic dyes from water by emulsion liquid membrane: Part 1: Membrane stability. *Sep. Purif. Technol.* **2008**, *62*, 636–641. [[CrossRef](#)]
63. Bourenane, S.; Samar, M.E.-H.; Abbaci, A.J.A.C.S. Extraction of cobalt and lead from waste water using a liquid surfactant membrane emulsion. *Acta Chim. Slov.* **2003**, *50*, 663–675.

**Disclaimer/Publisher’s Note:** The statements, opinions and data contained in all publications are solely those of the individual author(s) and contributor(s) and not of MDPI and/or the editor(s). MDPI and/or the editor(s) disclaim responsibility for any injury to people or property resulting from any ideas, methods, instructions or products referred to in the content.